A Ring Resonator Based Wide-Band Band Pass Filter with Single Loaded Stub and Compact Structure

Zafar Bedar Khan and Huiling Zhao

Department of Electronics and Information, Northwestern Polytechnical University, Xian, 710072, P. R. China
zafarbedarkhan@mail.nwpu.edu.cn, zhhl@nwpu.edu.cn

Abstract ─ A compact and simple structure of a wide-band band pass filter (BPF) based on ring resonator (RR) topology with only one open circuited stub is proposed. The pass band characteristic of the RR is achieved by placing the output port co-axial to the input port, at a position along the resonator length with maximum electric field. Subsequently wide operating bandwidth is realized by controlling the length of loaded stub due to its degenerate modes. An analytical equation is proposed based on even-odd mode analysis of a simplified transmission line model centrally loaded with stub to theoretically predict the positions of transmission zeros. A cascaded structure of two stub-loaded RRs filter with improved out of band rejection is designed and fabricated at 3 GHz. The insertion loss (IL) and return loss (RL) are better than 1.7 dB and 12.3 dB with a 3-dB fractional bandwidth of 47%. The two transmission zeros at 2.26 GHz and 3.8 GHz show rejections better than 37 dB. Furthermore, the area of the filter is reduced by special placement of the open circuited stubs inside the rings. It is shown that the compact filter is 33% area efficient with comparable performance parameters.

Index Terms ─ Open circuited stub, ring resonator, transmission zeros, wide-band band pass filter.

I. INTRODUCTION

Band pass filter (BPF) is one of the most important passive devices used in modern communication systems for sharp out of band rejection, low insertion loss, desired wide pass-bands and low cost [1-3]. Microstrip dual-mode Ring Resonators (RR) with simple structure, having two transmission zeros near the pass band have been shown to be promising candidates for high performance wide-band BPF [3] incorporating the above mentioned characteristics. In general, two degenerated modes can be excited by introducing a perturbation element along an orthogonal plane of RR. To properly split these two modes, different perturbation elements with various configurations have been introduced in a ring resonator with respect to its two ports [4-17]. In [4], the two degenerate-mode frequencies of the stepped-impedance ring resonator are controlled through the length ratio of two line sections with different characteristic impedances. As simple perturbation elements, lumped capacitors are placed at the diagonal corners of a symmetrical ring in series and/or shunt formats [5-6]. Small patches and/or notches placed at the corners of square-loop [7], hexagonal-loop resonators [8] and narrow slots etched on ground plane underneath a symmetrical ring strip conductor [9] are other perturbation elements proposed in the literature. Many researchers have reported RR based design of wide-band BPFs [10-17]. In [10-12], RR based BPF design with relatively narrower fractional bandwidth (FBW) (10% ~ 11%) were presented. Owing to the coupled lines in the proposed designs in [10-11], the insertion loss (IL) was slightly higher at 2.3 dB and 2.4 dB respectively. Six and four-transmission zeros respectively were implemented in [13-14] at the cost of complex structures with discontinuities and coupling gaps. Moreover, the achieved fractional bandwidth (FBW) was around 20% and 21% respectively, which was less as compared to other reported works. The structure of RR based wide-band BPF reported in [15] allowed the tuning of the center frequency as well as the BW by tuning the voltage of varactors. The design required external voltage to be provided to three varactors through wires which may not prove viable at higher frequencies due to parasitic effects. Subsequently in [16], complementary split ring resonators with cascaded high pass and low pass filters were used to demonstrate wide-band BPF with improved FBW. The complex structure (with coupling gaps) on two layers of the substrate may be relatively difficult to manufacture as compared to a single sided micro-strip structure, for example reported in [17]. A wide-band BPF was introduced in [17] using RR and two stubs. The reported technique avoided mismatches due to no coupling gaps and thus a low insertion loss (IL) of better than 1.6 dB and a good FBW of 49.3% was achieved. Firstly, band-stop characteristics were realized by orthogonal placement of input/output ports on the ring resonator. Subsequently, two stubs were used to attain wide band pass characteristics of the structure owing to the degenerate modes of the stubs.

In this paper, it is established that comparable FBW

Submitted On: April 13, 2017
Accepted On: October 4, 2017

can be achieved from a single RR and a single loaded tuning stub making the BPF structure simpler and area efficient as compared to [17]. In Section IIA, the analytical investigation of the surface currents/voltages nulls and subsequent simulation is performed assuming transmission line model of the RR. Based on the analysis and simulation, instead of orthogonal placement (as established in [17]), co-axial placement of the input/ output ports is proposed with output port at the position of minimum current and maximum voltage implying maximum electric field. The proposed co-axial placement of the ports thus results in the band pass characteristic of the RR (circumventing the band-stop design step as suggested in [17]).

Subsequently, in Section IIB, a single open-circuited stub is demonstrated to be sufficient to achieve a wide-band response of the BPF owing to the degenerate modes induced by different stub lengths. The presented circuit is analytically solved and an equation is derived theoretically predicting the transmission zeros (TZs). In Section IIC, a cascaded arrangement of two RR with one stub each is designed and fabricated which further improves the out of band rejection. Furthermore, in Section IID, it is shown that, the compact placement of the stub itself inside the RR of the cascaded structure proves to be area efficient maintaining comparable performance. Compact wide-band BPF with two cascaded RR and specially placed stubs is also designed and fabricated. The measurements show good conformance with the simulated response at the center frequency (CF) of 3 GHz.

II. PROPOSED METHODOLOGY FOR FILTER DESIGN

The following analysis is performed for a fundamental design frequency of 3 GHz. A substrate with a dielectric constant of 2.2 and thickness 0.8 mm, and system impedance of 50Ω is considered for all calculations. Advance design system (ADS) software is used for the simulation work. All the measurements were performed on Agilent's PNA model no. E8363B.

A. Band pass characteristic of RR using co-axial feed lines

A ring resonator can be analyzed by an equivalent straight transmission line as shown in Fig. 1 (a). Knowing the distribution of voltage and current along this straight resonator makes it possible to decide the positions of the input/output feed lines which ensure the odd or even mode excitation. For the resonator shown in Fig. 1 (a), the input admittance can be given as:

$$Y_{in} = jY_0 \tan\theta . \quad (1)$$

For resonance condition it can be deduced that,

$$\theta = n\pi$$
$$l_r = \frac{n\lambda_g}{2}, \quad (2)$$

where θ is the electrical length, lr is the physical resonator length and λg is the guided wavelength at the resonance frequency. From (1) it can further be inferred that the voltage and current along the resonator length are functions of cosθ and sinθ respectively.

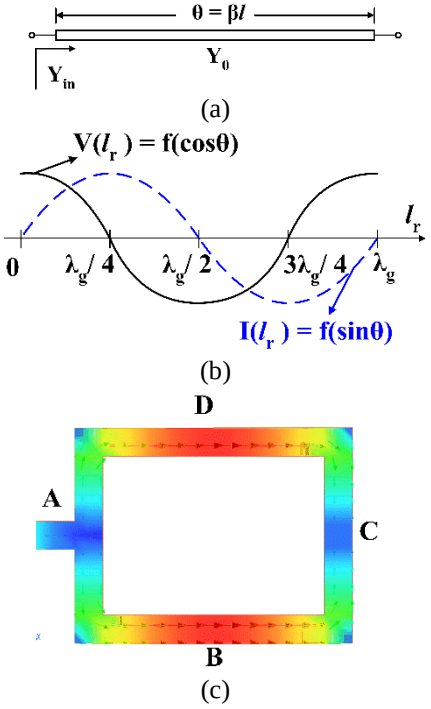

Fig. 1. (a) Straight transmission line resonator, (b) voltage and current waveform along the resonator length lr = λg, and (c) simulated surface current distribution on the RR at fundamental frequency.

Now for a resonator with a length of one full guided wavelength (lr = λg) [3] (n=2 from (2)), the voltage and current nulls along the resonator length at fundamental frequency are plotted in Fig. 1 (b). Simulated surface current on RR (formed by folding the straight resonator in Fig. 1 (a)) is shown in Fig. 1 (c). Voltage nulls are observed at position 'B & D' (corresponding to (λg /4) and (3λg /4) in Fig. 1 (b)) due to maximum current (arrows shown in red color in Fig. 1 (c)). Current nulls are at 'A & C' (corresponding to 0 and (λg /2) in Fig. 1 (b)) due to maximum voltage. This gives a very clear idea that fundamental frequency or any odd mode resonance cannot be tapped at point 'B' (or 'D'), thus band stop characteristic is expected as established in [17]. Conversely, band pass characteristic of the RR

is expected at point 'C' due to presence of maximum electric field at the fundamental resonance frequency.

The proposed co-axial feed lines (at α = 0°) are placed at 'A & C' without any coupling gap as shown in Fig. 2 (a). The simulated and measured S-parameter response is depicted in Fig. 2 (b). As evident, the co-axially placed feed lines give a band pass response centered at the fundamental design frequency of 3 GHz.

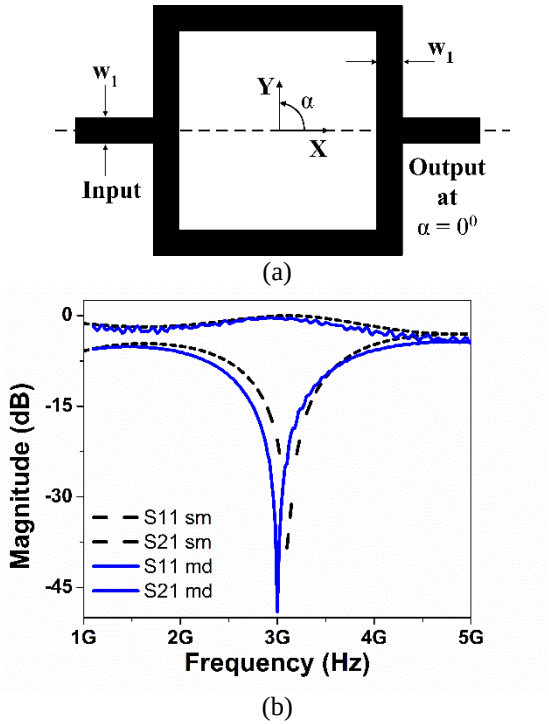

Fig. 2. (a) RR with co-axial feed lines, and (b) S-parameters response (sm = simulated, md = measured).

B. Wide-band characteristic by using one stub

It is an established fact that the frequency response of an RR can be varied by controlling the length of the loaded stub [3, 11]. Furthermore, the impedance of the stub is kept higher than the RR for better return loss (RL) [17]. The concept is employed here to get the wide-band response of the co-axially fed RR at 3 GHz. For the purpose, the stub may be loaded at position 'B or D' (refer to Fig. 1 (c)). Figure 3 (a) shows a stub with length ls = λg /4 loaded at position 'D' of the co-axially fed RR. Please note that the stub length (ls) is designed at the fundamental design frequency for an optimized impedance of 64Ω.

Simulated frequency response with varying stub length is depicted in Fig. 3 (b). Degenerate modes can be observed with the introduction of the stub. It is clearly seen that with increasing length of the stub (ls), the frequency BW is widened with the best response at ls = λg /4. The final dimensions (in mm) of the RR filter in Fig. 3 (a) at 3 GHz for 50Ω system were taken as: lr = λg = 73, w_1 = 2.44, ls = 18.43, w_2 = 1.65. Widths of both the feed lines were kept same as w_1.

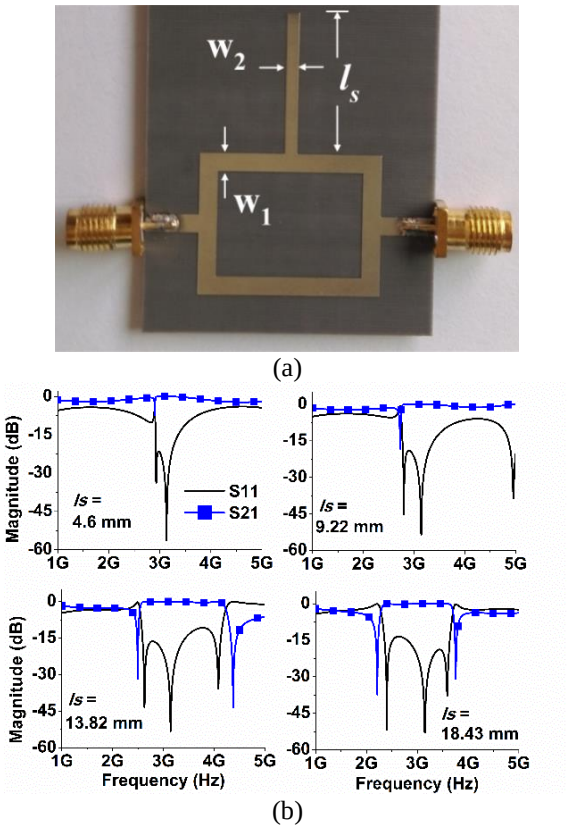

Fig. 3. (a) Fabricated RR with single loaded stub, and (b) simulated S-parameters with varying stub length ls.

1) Theoretical Analysis for Determination of Transmission Zeros

As stated earlier and shown in Fig. 3 (b), the RR based BPF has a sharp skirt due to presence of (at least) two transmission zeros. Lower and higher transmission zero (TZ) frequencies (f_{TZ1} & f_{TZ2} respectively) are theoretically predicted using even and odd mode analysis of the RR BPF structure with one open sub shown in Fig 3 (a). For the purpose, again a simple transmission line centrally loaded with an open stub is adopted as shown in Fig. 4 (a). The central plane (AA') in Fig. 4 (a) is equivalent to an electric and a magnetic wall when the odd- and even-modes are excited respectively. Therefore, following the odd mode and even mode half circuits shown in Figs. 4 (b) & (c) respectively, the admittance equations can be derived as:

$$Y_{ino} = \frac{Y_0}{j \tan(\theta/2)} \quad \text{(for odd mode)}, \tag{3}$$

$$Y_{in\,e} = jY_0 \frac{2\tan(\theta/2)+R\tan(k\theta)}{2-R\tan(\theta/2)\tan(k\theta)} \quad \text{(for even mode)}, \tag{4}$$

where $Y_{in\ o}$ and $Y_{in\ e}$ are the odd and even mode

admittance respectively. R is the impedance ratio defined as Zs/Z_0 (or admittance ratio Z_0/Zs), whereas $k = \theta s / \theta$ is defined as electrical length ratio. Since for this work, $Z_0 = 50\Omega$, $Zs = 64\Omega$, $\theta s = \pi/4$ and $\theta = 2\pi$ has been chosen based on the presented analysis, therefore R = 0.78 and k = 1/8.

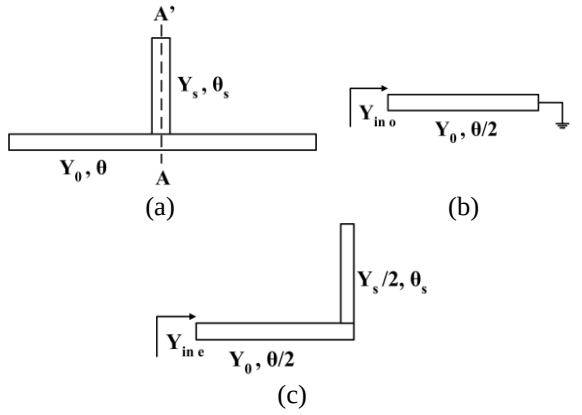

Fig. 4. (a) A simple transmission line model with centrally laoded open stub, (b) even mode circuit, and (c) odd mode circuit.

Please note from (3) that at resonant condition, odd mode frequency can be found out which corresponds to the center frequeny (CF). That is at Yin o = 0, $\theta = n\pi$, (and since n was selected as 2 in Subsection IIA), the center (odd mode) frequency is clculated to be 2.99 GHz which is almost the design frequency considered in this work. Moreover transmission zeros can be predicted by setting S21 equation equal to zero, as,

$$S21 = |Y_{in\,o}| - |Y_{in\,e}| = 0 . \quad (5)$$

Using (3) and (4) in (5), and after some manipulations, following equation can be derived:

$$S21 = |Y_{in\,o}| - |Y_{in\,e}| = \frac{1}{\tan(\theta/2)} - R\tan(k\theta) - 2\tan(\theta/2) = 0 . \quad (6)$$

Equation (6) is solved and the result is plotted against normalized frequency (f/f_0, where f_0 = CF = 3 GHz) on the x-axis as shown in Fig. 5. The lower and higher TZ frequencies f_{TZ1} and f_{TZ2} are respectively predicted to be at $0.77f_0$ (f_{TZ1} = 2.3 GHz) and $1.2f_0$ (f_{TZ2} = 3.6 GHz). Although two more TZs are theoratically expected at about 0.57 GHz and 5.1 GHz, but for our work, we are only interested in the TZs nearest to the CF.

2) Practical Demonstration

Simulated and measured responses of this asymmetric structure with one RR and a loaded stub are shown in Fig. 6. Good agreement is observed. The 3-dB FBW is 47% (from 2.32-3.73 GHz). The measured IL and RL are better than 1.6 dB and 13 dB respectively. Two transmission zeros at 2.26 GHz and 3.8 GHz give a rejection of -24.17 dB and -23.53 dB respectively. The difference of the theoretical and experimental values of f_{TZ1} and f_{TZ2} are noted to be 1.7% and 5.5%, being reasonably acceptable. It may be noted here that the area of the designed BPF is 14.8 cm^2 (3.7 cm × 3.79 cm), which as compared to an area of 22 cm^2 (4.4 cm × 5.0 cm) (if implemented at the same design frequency by method given in [17]), gives an area reduction of 48%.

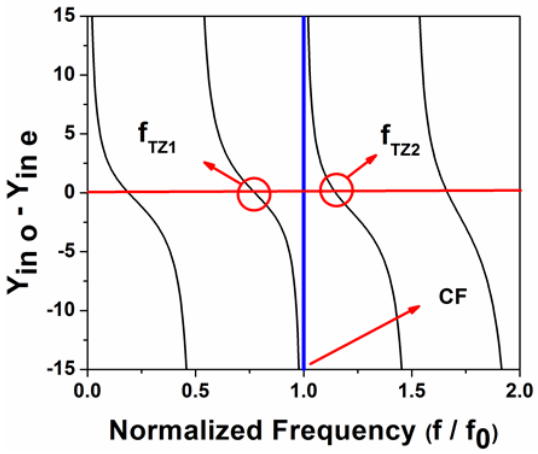

Fig. 5. Theoretically predicted transmission zeros plotted against frequency normalized at CF = 3 GHz.

C. Cascaded wide-band BPF (CWBF)

Out of band rejection of the transmission zeros of the RR with single stub can be improved by cascading two or more such structures. In this work only two BPFs of Fig. 3 (a) were cascaded to prove the point. Figure 7 (a) shows the manufactured cascaded wide-band RR BPF with an area of 34.02 cm^2 (8.1 cm × 4.2 cm). Note that the distance (d) between the two RR was optimized at about $\lambda g/4$, i.e., d = 18.43 mm. It can be seen in Fig. 7 (b) from the measured response that the transmission zeros at 2.26 GHz and 3.8 GHz are now at -55.5 dB and -37 dB giving a considerable improvement as compared to measured response in Fig. 6.

Here the 3-dB FBW is 46.5% which is close to 47% as in previous section. The slight variation may be due to manufacturing tolerance. The IL and RL are better than 1.7 dB and 12.3 dB respectively. The reported area of the CWBF (34.02 cm^2) is about 36% less than if it was implemented with the methodology in [17] at 3 GHz (in the latter case the area comes out to be 53.68 cm^2 (8.8 cm × 6.1 cm)). Please note that the area reduction given by the implemented simple structures shown in this sub-section and the previous one is quite significant compared to [17].

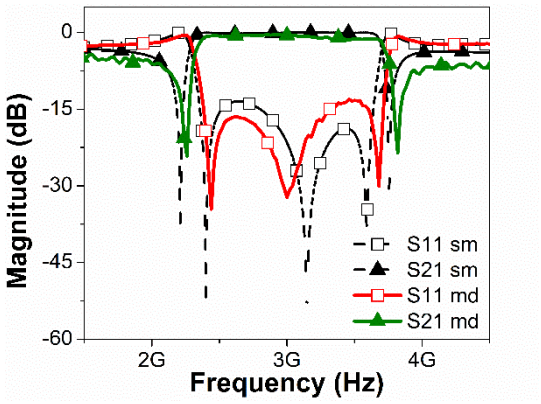

Fig. 6. S-parameters response of fabricated RR with single loaded stub with $l_s = \lambda_g/4$ (sm = simulated, md = measured).

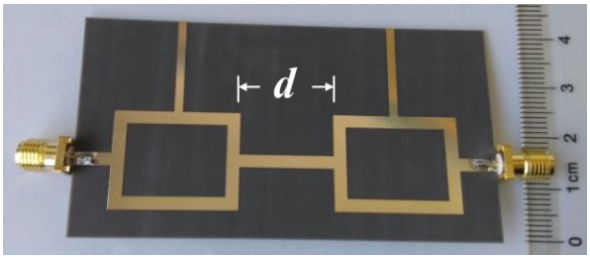

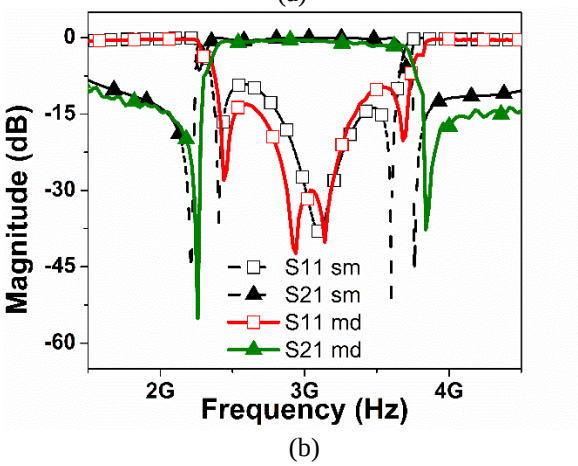

Fig. 7. (a) Fabricated cascaded RR with loaded stubs, and (b) S-parameters response (sm = simulated, md = measured).

D. Compact cascaded wide-band BPF (CCWBF)

As shown in Fig. 8 (a), the open stubs are placed inside the RR in order to save area without much compromise on the performance. The internal couplings of the stub with the RR were ignored for this analysis and the distance (d) between the two RRs was taken to be 18.43 mm. The area of the CCWBF came out to be 8.1 cm × 2.8 cm giving an improvement of about 33% as compared to the one shown in Fig. 7 (a).

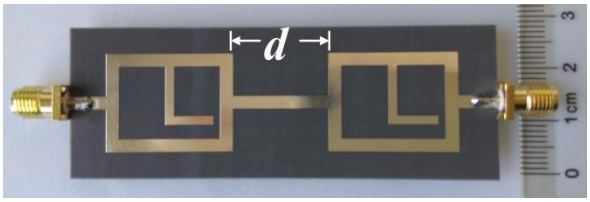

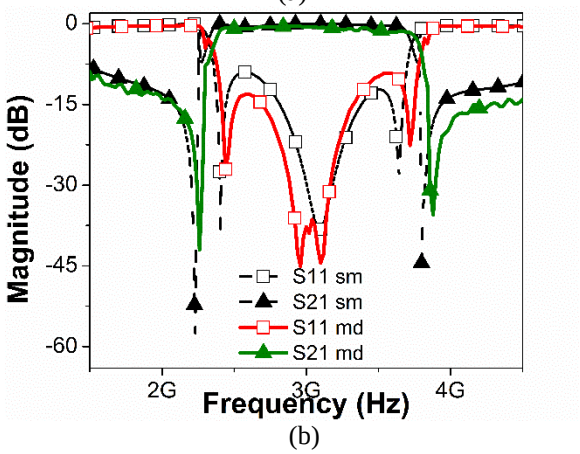

Fig. 8. (a) Fabricated compact cascaded RR with loaded stubs, and (b) S-parameters response (sm = simulated, md = measured).

The S-parameter response of the CCWBF is shown in Fig. 8 (b). It is evident that the performance of the compact cascaded BPF is comparable to the cascaded BPF shown in Fig. 7 (b). The measured transmission zeroes at 2.28 GHz and 3.88 GHz are at -42 dB and -37 dB respectively. Overall the IL and RL are better than 1.8 dB and 11.2 dB with a difference of about 6% and 8% respectively as compared to cascaded filter. The 3-dB FBW came out to be 47.3%. Slight shift in the pass-band edge frequencies may be contributed to the internal couplings of the stub with RR and/or manufacturing tolerance which are reported to be 2.35 - 3.77 GHz.

E. Comparison with previous works

A comparison of the proposed technique with previously presented work is summarized in Table 1. It may be noted that as compared to previous work, the proposed methodology presents a simplified structure with only single stub operational over a comparable or better FBW with low IL. It is also evident that the proposed wide band filter has a very compact area which is an added advantage of the proposed technique. Of course if sharp roll-off is a critical design parameter, designs proposed in [12-14] may be adopted with limited BW. But if it is not the case, then the proposed designed offers reasonably good performance parameters over a wide bandwidth in less area.

Table 1: Comparison of proposed technique with previous work

Works	Parameters					
	Structure	FBW (%)	$\|S_{11}\|$ (dB)	$\|S_{21}\|$ (dB)	Tx[a] Zeros	Area
[10]	Triangular RR+2 coupled transmission lines	11.2	> -10	2.3	2	>1.15λg × 0.5λg
[11]*	RR + coupled transmission lines	10	-40 (at CF)	2.4	3	~0.5λg × 0.5λg
[12]**	2RR + 2 open Stubs	10.7	-40 (at CF)	-1.63	6	Not given exactly, but large than 0.5λg × 0.5λg
[13]	RR+ 2 transmission lines + 2stubs	20.6	> -12.5	< -2.2	6	1.06λg × 0.61λg
[14]	RR+ 2 transmission lines + 2stubs	21.9	> -12.5	< -2	5	~0.76λg × 0.33λg
[17]	RR + 2 stubs	49.3	> -13.3	< -1.6	2	0.42λg × 0.29λg
This work	RR + single stub	47	> -12.3	< -1.7	2	0.1λg × 0.04λg

[a] Transmission;
* Only BPF with two cascaded basic cells is considered;
** Only passive filter is considered.

III. CONCLUSION

Based on the voltage and current analysis along the ring resonator length, a co-axial scheme of feed lines is proposed which ensures the band-pass characteristic of the RR. The wide-band response was achieved by loading the RR with a single λg /4 open stub. The structure of the RR wide-band BPF was simplified and made area efficient as compared to [17] owing to the co-axial placement of feed lines and only one stub. The theoretical prediction of the TZs through presented analysis agrees well with the measured values with error less than 5.5%. Subsequently, cascaded (CWBF) and compact cascaded (CCWBF) wide-band BPF were designed and fabricated with latter showing an area reduction of 33% due to the special placement of the stub inside the RRs. The cascaded structure improved the out of band rejection with two transmission zeros at 2.26 GHz and 3.8 GHz with rejection better than 37 dB. The achieved 3-dB FBWs of the designed cascaded/ compact cascaded filters were 46% / 47.3% with an IL and RL better than 1.7 dB / 1.8 dB and 12.3dB / 11.2 dB respectively.

REFERENCES

[1] L. Zhou, Y. Z. Yin, W. Hu, and X. Yang, "Compact bandpass filter with sharp out-of-band rejection and its application," *Applied Computational Electromagnetics Society (ACES) Journal*, vol. 32, no. 3, pp. 249-255, Mar. 2017.

[2] A. K. Tiwary and N. Gupta, "Compact wide band printed filter with improved out-of-band performance," *Applied Computational Electromagnetics Society (ACES) Journal*, vol. 29, no. 3, pp. 224-230, Mar. 2014.

[3] K. Chang, *Microwave Ring Circuits and Antennas*. Wiley, New York, 1996.

[4] M. Matsuo, H. Yabuki, and M. Makimoto, "Dual-mode stepped impedance ring resonator for band-pass filter applications," *IEEE Trans. Microw. Theory Techn.*, vol. 49, no. 7, pp. 1235-1240, 2001.

[5] B. T. Tan, S. T. Chew, M. S. Leong, and B. L. Ooi, "A dual-mode bandpass filter with enhanced capacitive perturbation," *IEEE Trans. Microw. Theory Techn.*, vol. 51, no. 8, pp. 1906-1910, 2002.

[6] M. F. Lei and H. Wang, "An analysis of miniaturized dual-mode bandpass filter structure using shunt-capacitance perturbation," *IEEE Trans. Microw. Theory Techn.*, vol. 53, no. 3, pp. 861-867, 2005.

[7] A. Gorur, "Description of coupling between degenerate modes of a dual-mode microstrip loop resonator using a novel perturbation arrangement and its dual-mode bandpass filter applications," *IEEE Trans. Microw. Theory Techn.*, vol. 52, no. 2, pp. 671-677, 2004.

[8] R. J. Mao and X. H. Tang, "Novel dual-mode bandpass filters using hexagonal loop resonators," *IEEE Trans. Microw. Theory Techn.*, vol. 54, no. 9, pp. 3526-3533, Sep. 2006.

[9] B. T. Tan, J. J. Yu, S. T. Chew, M. S. Leong, and B. L. Ooi, "A miniaturized dual-mode ring band-pass filter with a new perturbation," *IEEE Trans. Microw. Theory Techn.*, vol. 53, no. 1, pp. 343-348, 2005.

[10] J. S. Hong and S. Li, "Theory and experiment of dual-mode microstrip triangular patch resonators and filters," *IEEE Trans. Microw. Theory Techn*.,

vol. 52, no. 4, pp. 1237-1243, Apr. 2004

[11] M. Salleh, G. Prigent, O. Pigaglio, and R. Crampagne, "Quarter-wavelength side-coupled ring resonator for bandpass filters," *IEEE Trans. Microw. Theory Techn.*, vol. 56, no. 1, pp. 156-162, Jan. 2008.

[12] R. Gomez-Garcıa, J. I. Alonso, and D. Amor-Martin, "Using the branch line directional coupler in the design of microwave bandpass filters," *IEEE Trans. Microw. Theory Techn*., vol. 53, pp. 3221-3229, 2005.

[13] W. Feng, X. Gao, W. Che, and Q. Xue, "Bandpass filter loaded with open stubs using dual-mode ring resonator," *IEEE Microw. Wireless Compon. Lett*., vol. 25, no. 5, pp. 295-297, 2015.

[14] K. Deng, Z. Chen, and W. Feng, "Bandpass filter with four transmission zeros using dual-mode ring resonator," *Progress in Electromagnetics Research PIER Letters*, vol. 56, pp. 129-132, 2015.

[15] H. Zhu and A. Abbosh, "Compact tunable bandpass filter with wide tuning range using ring resonator and short-ended coupled lines," *Electron. Lett*., vol. 51, no. 7, pp. 568-570, 2015.

[16] M. Oliaei, M. Tayarani, and M. Karami, "Compact microstrip bandpass filter improved by DMS and ring resonator," *Progress In Electromagnetics Research PIER Letters*, vol. 45, pp. 7-12, 2014.

[17] L.-H. Hsieh and K. Chang, "Compact, low insertion-loss, sharp-rejection, and wide-band microstrip bandpass filters," *IEEE Trans Microw. Theory Tech*., vol. 51, no. 4, pp. 1241-1246, 2003.

Zafar Bedar Khan received his B.E. (Avionics) degree from National University of Sciences and Technology, Pakistan and M.S. (Electronics & Comm.) degree from Hanyang University, South Korea in 2002 and 2010 respectively. Khan has been working as a Research Engineer in an R&D organization in Pakistan in the field of RF Front-end Design. He is currently pursuing his Ph.D. degree in Northwestern Polytechnical University, Xian, China. His research interests include RF passive component design for RF front-end application in Radar and communication systems.

Huiling Zhao received her Ph.D. degree in Circuit and System from Northwestern Polytechnical University, Xian, China in 2002. Zhao is currently a Professor in the Department of Electronics and Information, Northwestern Polytechnical University, China. She has been a Visiting Associate Professor in the Duke University, USA from 2006 to 2007. Zhao's main research interests include optimization algorithm development for beam forming, computational electromagnetics, microwave and millimeter wave circuit and antenna design.